

# Non-Markovian polariton dynamics in organic strong coupling

Antoine Canaguier-Durand<sup>1,a</sup>, Cyriaque Genet<sup>1</sup>, Astrid Lambrecht<sup>2,b</sup>, Thomas W. Ebbesen<sup>1</sup>, and Serge Reynaud<sup>2</sup>

<sup>1</sup> ISIS and icFRC, Université de Strasbourg and CNRS (UMR 7006), 8 allée Gaspard Monge, 67000 Strasbourg, France

<sup>2</sup> Laboratoire Kastler Brossel, UPMC-Sorbonne Universités, CNRS, ENS-PSL Research University, Collège de France, 4 place Jussieu, 75002 Paris, France

Received 21 July 2014 / Received in final form 22 October 2014

Published online 21 January 2015 – © EDP Sciences, Società Italiana di Fisica, Springer-Verlag 2015

**Abstract.** Strongly coupled organic systems are characterized by unusually large Rabi splitting, even in the vacuum state. They show the counter-intuitive feature of a lifetime of the lower polariton state longer than for all other excited states. Here we build up a new theoretical framework to understand the dynamics of such coupled system. In particular, we show that the non-Markovian character of the relaxation of the dressed organic system explains the long lifetime of the lower polariton state.

## 1 Introduction

Over the past 15 years, light-matter strong coupling has been studied extensively with organic materials [1–13] which can display very large splitting of the two hybrid light-matter states, also known as the polariton states. Recently, optical resonances with small mode volumes such as Fabry-Perot nanocavities or surface plasmons have been used to achieve the so-called ultra-strong coupling where the Rabi splitting approaching  $\sim 1$  eV becomes a significant fraction of the electronic transition energy [14,15]. For such large splittings, changes in bulk properties are observed, as already shown for the work-function [16] and the ground state energy [17]. It has also been noticed over the years that the lifetime of the lowest polariton state, denoted  $C^-$ , is much longer than the lifetime of the photon in the cavity mode [18–25]. In recent experiments using resonant excitation, this  $C^-$  lifetime has even been shown to be longer than that of the bare excited molecules [26,27].

These properties are counter-intuitive in the conventional picture where the dynamic properties of the coupled states are directly determined from those of the bare ones [28]. In the so-called Markov approximation, the effects of coupling and relaxation are simply added to each other in the master equation which describes the evolution of the system. It follows that the relaxation rates in the diagram of dressed states are obtained from those of bare states through a mere change of basis [29]. In the ultra-strong coupling limit in particular, the low- and high-energy dressed states  $C^-$  and  $C^+$  contain identical proportions of the bare states and their lifetimes are thus expected to be equal to each other. The experimental observation of very different lifetimes for these two dressed

states proves that the relaxation of the dressed system is deeply influenced by the strong coupling [30].

In the present article, we build up a new theoretical framework to understand the dynamics of ultra-strongly coupled organic molecules. We develop a non-Markovian approach within which the relaxation of molecules is studied in the diagram of dressed states resulting from the strong coupling [30]. This new view on strongly coupled organic materials allows us to establish a connection between the large value of Rabi splitting and two salient features seen in experiments, namely the unexpected long lifetime of the lower dressed state  $C^-$  and the asymmetry in lifetimes between the dressed  $C^+$  and  $C^-$  states. The predictions from this new point of view agree with detailed observations performed on strongly coupled organic systems [31].

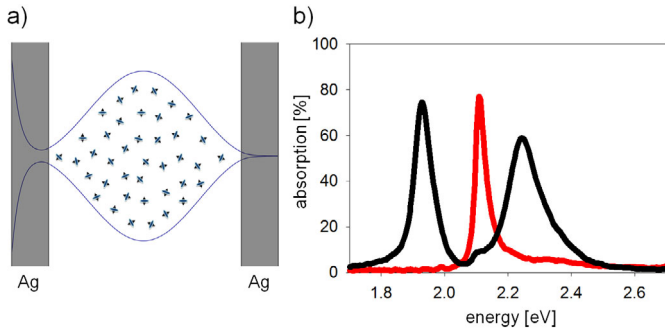
## 2 Non-Markovian dynamics

Figure 1 illustrates the case of organic molecules strongly coupled to a Fabry-Perot cavity mode. The organic molecules are doping a host polymer matrix at 0.1 to 0.01 molar concentration (mole per litre). Qualitatively, this corresponds to typical intermolecular separation distances of the order or larger than 3 nm within the host matrix, so that Förster-type energy transfer is expected to dominate over other intermolecular transfer mechanisms [32]. Absorption spectra on the right-hand side of the figure shows the effect of strong coupling which splits the molecular resonance in the coupled system (dark curve), as compared to the uncoupled one (red curve).

We stress here that the widths of the molecular absorption peaks are not directly related to the intrinsic molecular lifetimes, due to inhomogeneous broadening and vibrational manifold. Inhomogeneous broadening is due to distribution of orientations, locations and micro-environment of the organic molecules in the matrix.

<sup>a</sup> Present address: Institut Langevin, ESPCI ParisTech, PSL Research University, 1 rue Jussieu, 75005 Paris, France

<sup>b</sup> e-mail: astrid.lambrecht@lkb.ens.fr



**Fig. 1.** (a) Illustration of molecules coupled to the fundamental optical mode of a 145 nm thick Fabry-Perot cavity made of two 30 nm thick Ag mirrors. (b) Typical example of absorption spectrum of uncoupled (red line) and coupled (dark line) molecules. The data correspond to J-aggregate (TDBC) molecules dispersed in a polyvinyl alcohol (PVA) polymer host matrix inside the cavity sketched in (a) [27].

This feature is crucial for coupled and uncoupled organic molecules to coexist in the cavity in the model discussed further down, and it prevents one to draw conclusions about intrinsic lifetimes from the measured spectral features. These features are essentially the same for coupled and uncoupled molecules, since the optical coupling does not affect the associated motions. In addition, the host matrix behaves as a vibrational relaxation reservoir in thermodynamic equilibrium with both coupled and uncoupled molecules.

The vibrational reservoir spectra are characterized by a typical energy dispersion  $k_B T \simeq 25$  meV at room temperature, or equivalently a correlation time  $\tau_c \simeq \hbar/k_B T \simeq 25$  fs. The condition of validity of the Markov approximation [30] would be that the Rabi splitting  $\Omega_R$  be inefficient during the correlation time  $\Omega_R \tau_c \ll 1$ , that is equivalently  $\hbar \Omega_R \ll k_B T$ . This condition is clearly not met for ultra-strong coupling of organic molecules, where the Rabi splitting  $\hbar \Omega_R$  is much larger than  $k_B T$  [33,34]. We emphasize that this is different from the criterium for the ultra-strong coupling regime, which is a comparison between the Rabi splitting energy and the electronic transition energy [14].

At this point, a clear distinction must be made between inorganic and organic systems. While most organic materials are characterized by vibrational relaxation reservoirs, this is not necessarily the case for inorganic systems. Therefore, although Rabi splittings larger than  $k_B T$  have been measured at low temperature on inorganic systems, their relaxation dynamics do not necessarily involve non-Markovian effects because of this difference in properties of relaxation reservoirs. In the case of organic systems in contrast, relaxation is mainly driven by vibrational reservoirs, with a typical energy dispersion given by thermal energy. This implies that the system is necessarily in the non-Markovian regime, with relaxation strongly influenced by the coupling, as soon as  $\hbar \Omega_R \gg k_B T$ . Then, there is no reason to expect that the dressed states  $C^+$  and  $C^-$  have identical lifetimes, as it would be the case for ultra-strong coupling in the Markovian approximation. We will see be-

low that the hierarchy of lifetimes observed in experiments is naturally explained by the approach proposed in this paper.

In our case, each individual molecule is only weakly coupled to the electromagnetic mode of the cavity, and the strong coupling mechanism involves a collective excitation of an extremely large number of molecules coherently coupled to the single mode of the cavity. The strong coupling does not shield the molecules from intramolecular vibrational relaxation which explains the extremely low emission quantum yields, as observed experimentally, with vibrational relaxation rates at least 100 times larger than the radiative rate of  $C^-$ . For instance in the case of TDBC presented in Figure 1, the fluorescence quantum yield of  $C^-$ , angularly integrated, is found to be  $\sim 8 \times 10^{-3}$  (more numbers will be given below).

We build up below the new theoretical framework which naturally allows us to analyze such situations. We show in particular that the non-Markovian character explains the otherwise counter-intuitive long lifetime of the lower dressed state  $C^-$ . We stress at this point that a problem dominated by radiative relaxation would lead to different conclusions [29]. Note also that, in what follows, dark states which are formed in the coherent state manifold when coupling a large number of molecules to one cavity mode are ignored [33]. Nevertheless, their mere presence in the energy diagram also contributes to the non-radiative decay discussed further down.

### 3 Bare and dressed states

We consider uncoupled (U) and coupled (C) states as two populations in a dynamical equilibrium with the total concentration  $[M] = [U] + [C]$  fixed. This model amounts to consider the dynamical equilibrium inside the cavity between the two populations from a first-order kinetics point of view. Within such a point of view, uncoupled and coupled molecular populations coexist, at thermal equilibrium, with well-defined Gibbs free energy differences. As usual, predictions made by such a model have to be compared to experimental observations. To this aim, we have recently measured how the fraction of coupled molecules to the uncoupled ones increases with the Rabi splitting, confirming a central relation implied by the two-species thermodynamical approach [17].

It is worth keeping in mind that this model is a simplification of the actual complexity of the situation where there is a continuous distribution of molecules in the cavity mode with different positions, orientations of the molecular transition dipole moments with respect to the electric field of the cavity mode or environments which lead to spectral inhomogeneous broadening. It is an important task for future studies to go beyond this effective macroscopic approach in order to fully understand, from first principles, how interactions induced inside the cavity at the molecular scale lead to the distribution of coupled vs. uncoupled molecules which is observed in experiments.

The relevant states of the uncoupled molecules are, on the one hand, the ground and excited states of

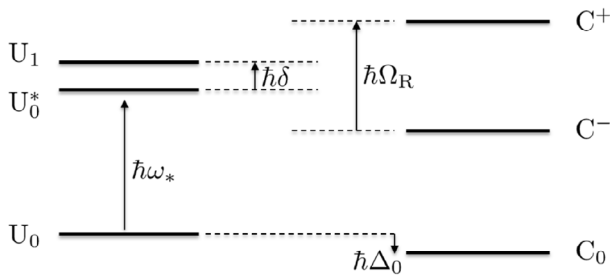


**Fig. 2.** Energy diagram of the bare states U and dressed states C of the “molecule+cavity” system. The energy difference between  $U_1$  and  $U_0^*$  is  $\hbar\delta$ , with  $\delta = \omega_1 - \omega_*$  the detuning between the frequency  $\omega_1$  of the cavity mode, and  $\omega_*$  that of the molecular transition. The Rabi splitting  $\hbar\Omega_R$  between the dressed states  $C^+$  and  $C^-$  and the energy shift  $\hbar\Delta_0$  of the ground state  $C_0$  are shown.

the molecule U and  $U^*$  and, on the other hand, the 0- and 1-photon states of the cavity. The states of the hybrid “molecule + cavity” system are denoted  $U_0$  for the ground state,  $U_1$  and  $U_0^*$  for the excited ones (see Fig. 2). The energy difference between the two excited states is:

$$\hbar\delta = \hbar\omega_1 - \hbar\omega_*, \quad (1)$$

with  $\omega_1$  the frequency of photons in the cavity mode and  $\omega_*$  the frequency of the molecular transition. The detuning  $\delta$  (as the Rabi coupling discussed in the next paragraph) has a single value in the simplified two-population model whereas it would have a distribution of values in a microscopic description.

The relevant states are similar for coupled and uncoupled molecules, with differences caused by the effects of the coupling. They are denoted  $C_0$ ,  $C_1$  and  $C_0^*$ , with the symbol C replacing U. The excited states  $C_1$  and  $C_0^*$  are coupled through the Rabi coupling  $2\nu$  which is not zero for the coupled molecules. Note that this Rabi splitting has a large value, though the cavity has a low quality factor  $Q$  and remains in low states with only 0 or 1 photon. This unusual feature is due to the already discussed fact that the cavity field is coupled to a giant dipole corresponding to the coherent superposition of an extremely large number of molecules.

The dressed states, denoted  $C^+$  and  $C^-$ , are obtained by diagonalizing the effect of the Rabi coupling between the states  $C_1$  and  $C_0^*$

$$\begin{aligned} C^+ &= \cos\theta C_0^* + \sin\theta C_1, \\ C^- &= \cos\theta C_1 - \sin\theta C_0^*, \end{aligned} \quad (2)$$

with the angle  $\theta$  defined by:

$$\tan(2\theta) = -2\frac{\nu}{\delta}, \quad 0 \leq 2\theta \leq \pi. \quad (3)$$

$C^+$  is defined to have a higher energy than  $C^-$  and the splitting between the two states is:

$$\Omega_R = \sqrt{\delta^2 + 4\nu^2}. \quad (4)$$

The projection factors in equation (2) are

$$\cos^2\theta = \frac{\Omega_R - \delta}{2\Omega_R}, \quad \sin^2\theta = \frac{\Omega_R + \delta}{2\Omega_R}. \quad (5)$$

When the coupling is much larger than the detuning ( $2\nu \gg |\delta|$ ), these projection factors are nearly equal  $\cos^2\theta \simeq \sin^2\theta \simeq 1/2$ .

All molecular states are connected in the molecular hamiltonian so that the splitting of  $C^+$  and  $C^-$  has consequences on the other states. This causes in particular a downward shift  $\hbar\Delta_0$  of the position of the ground state  $C_0$  [14,17,35]. At resonance (zero detuning), the Rabi splitting is twice the coupling strength (see Eq. (4)), with gives  $2\nu \sim 1$  eV. With a distance between the ground and excited states  $\hbar\omega^* \sim 2$  eV, the  $\hbar\Delta_0$  shift cannot be neglected. A naive expectation  $\nu^2/(2\hbar\omega^*)$  from second order perturbation theory leads to a value consistent with the result of recent measurements  $\hbar\Delta_0 \sim 0.1$  eV. As this shift changes the energy differences between the states of uncoupled and coupled molecules, it can indeed be measured in a thermodynamic approach as the standard Gibbs free energy difference between the ground states of the uncoupled and coupled molecules [17].

## 4 Cavity relaxation processes

We now discuss the radiative relaxation processes which correspond to emission of a photon by the cavity with the molecular state unaffected. The basis of the method is the application of Fermi’s golden rule to dressed states [29].

For the uncoupled molecules, there is only one relaxation channel corresponding to the transition  $U_1 \rightarrow U_0$ . Simple rate equations describe the evolution of the populations  $[U_1]$  and  $[U_0]$  due to this process

$$\frac{d[U_1]}{dt} = -\frac{d[U_0]}{dt} = -\Gamma_{U_0U_1}[U_1], \quad (6)$$

and they preserve the sum of the two populations. The transition rate  $\Gamma_{U_0U_1}$ , defined for the transition  $U_1 \rightarrow U_0$ , is the product of a reduced rate  $\gamma$  and a spectral density of optical modes evaluated at the frequency of the transition. Absorption rate on the same transition is the product of the spontaneous emission cross section  $\sigma_{U_0U_1}$  by a photon flux  $\Phi_{U_0U_1}$  at the relevant frequency

$$\frac{d[U_1]}{dt} = A_{U_1U_0}[U_0], \quad A_{U_1U_0} = \sigma_{U_0U_1}\Phi_{U_0U_1}. \quad (7)$$

Note that the low  $Q$  factor favors absorption events in the cavity and thereby strong coupling.

For the coupled states, there are two radiative transition channels  $C^\pm \rightarrow C_0$  with rate equations

$$\frac{d[C^\pm]}{dt} = -\Gamma_{C_0C^\pm}[C^\pm]. \quad (8)$$

The rates are proportional to squared projection factors  $\Gamma_{C_0C^+} \propto \sin^2\theta$  and  $\Gamma_{C_0C^-} \propto \cos^2\theta$ , and to the spectral

densities of optical modes at the transition frequencies. As these frequencies differ from the bare one, the values of the emission and absorption rates differ from the expectations deduced from the Markov approximation.

In other words, the effect of strong coupling is studied on the diagram of dressed states with the relaxation processes described in terms of relaxation rates associated with the dressed transitions. If it were translated in terms of a master equation on the bare states, our approach would involve typical non-Markovian memory kernels (see for example [30]). Accordingly, it involves more parameters than a Markovian framework where the relaxation would be discussed by relaxation parameters defined on the bare molecules. In the dressed approach, the extra parameters are just the relaxation rates associated with the dressed transitions, with the advantage of naturally describing the large difference of lifetimes of the lower and upper polariton states (see below).

We note that the thermodynamical equilibrium is only slightly modified by the absorption processes. The total population of excited states does not exceed a fraction of the order of  $10^{-7}$  in the case of static spectroscopic experiments ( $\sim 10^{-2}$  for pump-probe measurements) so that the depletion of ground states remains negligible. This means that the populations  $[U_0]$  and  $[C_0]$  remain close to their values in vacuum and also explains why stimulated emission processes can be disregarded.

## 5 Vibrational relaxation processes

We now study vibrational relaxation processes which are the dominant relaxation mechanism for organic molecules. They correspond to internal conversion of energy via a rapid cascade down the vibrational ladder of the molecule. Typical organic molecules used in strong-coupling experiments have over 100 fundamental vibration modes.

Another non-radiative relaxation process is the Förster energy transfer between different molecules with conservation of energy. Well known in molecular photophysics [32], these processes correspond to a transfer of excitation due to Förster dipole-dipole coupling between molecules over distances of a few nm to a few tens of nm. The energy excess, required for energy conservation, is dissipated by a vibrational cascade down to the lowest level of the corresponding electronic multiplicity, as sketched on Figure 3. Though they involve Coulomb interaction, these energy transfer mechanisms, based on near-field dipole-dipole interactions, are often described as non-radiative as they do not couple to the free radiation field. It is also worth noting that, at the small intermolecular distance scales where they occur, they are expected not to perturb significantly the coherence of the collective dipole.

We do not enter into a detailed microscopic description of these processes, well-known in molecular science, which leave the cavity state unaffected. We give qualitative descriptions which are sufficient for our purpose. A crucial feature in our case is that the thermal energy  $k_B T$  is much smaller than energy differences, so that downward transitions are dominant. The only exception to this rule

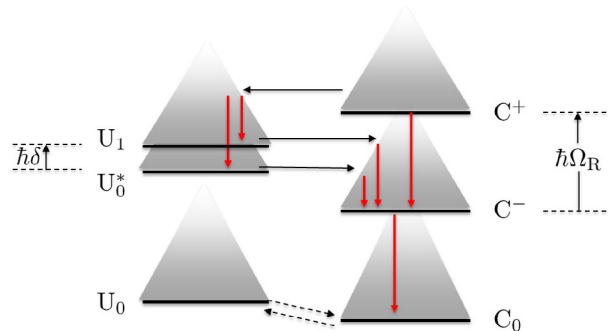


**Fig. 3.** Schematic representation of uncoupled U and coupled C states in the non-Markovian regime. The vibrational ladders associated with each molecular configuration are represented in grey shadows and the non-radiative relaxation paths as red vertical arrows. Transitions occurring between uncoupled and coupled molecules are represented by horizontal black arrows.

is the case of transitions between ground states which correspond to a smaller energy shift  $\hbar\Delta_0$  and determine the thermodynamical equilibrium of the ground states of the coupled and uncoupled molecules [17].

For uncoupled states, there is only one non-radiative transition  $U_0^* \rightarrow U_0$ . As previously, this process is described by a rate equation

$$\frac{d[U_0^*]}{dt} = -W_{U_0 U_0^*} [U_0^*]. \quad (9)$$

The rate  $W_{U_0 U_0^*}$  is the product of a reduced rate  $w^*$  by a spectral density  $\mathcal{S}$  which represents the coupling of the two vibronic multiplicities and depends on the energy difference. This reduced rate is relatively small as this energy difference is much larger than  $k_B T$ . For coupled states, there are similar transitions  $C^\pm \rightarrow C_0$

$$\frac{d[C^\pm]}{dt} = -W_{C_0 C^\pm} [C^\pm], \quad (10)$$

with  $W_{C_0 C^+}$  and  $W_{C_0 C^-}$  proportional to  $\cos^2 \theta$  and  $\sin^2 \theta$ , respectively.

There exists one relaxation channel which is opened by the strong coupling and could never be seen in the absence of this effect. It corresponds to the transition between the dressed excited states  $C^+ \rightarrow C^-$

$$\frac{d[C^+]}{dt} = -W_{C^- C^+} [C^+], \quad (11)$$

with a rate proportional to  $\cos^2 \theta \sin^2 \theta$ . This new channel, with a maximal rate when  $\cos^2 \theta \simeq \sin^2 \theta \simeq 1/2$ , is very similar to the collision-induced transitions studied in reference [30]. As the energy difference is smaller, the rate is larger than for transitions studied in the preceding paragraph.

We come now to a second category of transitions occurring between coupled and uncoupled molecules schematized in Figure 3. Such transitions are observed experimentally as energy transfer processes with well defined signatures [22,27]. In the study of ground states,

we consider reverse transitions  $C_0 \rightarrow U_0$  and  $U_0 \rightarrow C_0$  because the energy difference  $\Delta_0$  is not so large with respect to  $k_B T$ . These transitions produce the thermodynamical equilibrium between populations of coupled and uncoupled molecules

$$\frac{[C_0]}{[U_0]} = \exp \frac{\hbar \Delta_0}{k_B T}. \quad (12)$$

This equilibrium favors coupled molecules for a downward shift  $\hbar \Delta_0 > 0$  of the coupled state.

For similar transitions between the excited states of coupled and uncoupled molecules, energy differences are large, and we consider only downward transitions  $C^+ \rightarrow U_1$ ,  $U_1 \rightarrow C^-$ ,  $C^+ \rightarrow U_0^*$ ,  $U_0^* \rightarrow C^-$ . The rates  $W_{U_1 C^+}$ ,  $W_{C^- U_1}$ ,  $W_{U_0^* C^+}$ ,  $W_{C^- U_0^*}$  are respectively proportional to  $\sin^2 \theta$ ,  $\cos^2 \theta$ ,  $\cos^2 \theta$  and  $\sin^2 \theta$  and to spectral densities at the relevant frequencies. Hence, they can only be calculated on the diagram of dressed states and are not determined by rates known for bare molecules. This situation, typical for a non-Markovian regime, is in sharp contrast with the Markov approximation where the downward and upward rates would be similar.

## 6 Orders of magnitude

Magnitudes of the various rates are known from the experiments (see for instance [27]). The largest rate corresponds to the radiative transition between uncoupled states  $\Gamma_{U_0 U_1}$ . Given the low quality-factor of the cavity ( $Q \sim 10$ ), the radiative lifetime of the cavity mode is as short as 25 fs. This leads to a radiative rate as high as  $\Gamma_{U_0 U_1} \sim 4 \times 10^{13} \text{ s}^{-1}$ , which is strongly favored by the cavity. In particular it is much larger than the fluorescence rate which is of the order or smaller than  $10^{10} \text{ s}^{-1}$ .

Large values are also obtained for non-radiative transition rates between excited states  $W_{C^- C^+}$ ,  $W_{U_1 C^+}$ ,  $W_{U_0^* C^+}$ ,  $W_{C^- U_1}$ ,  $W_{C^- U_0^*} \sim 10^{13} \text{ s}^{-1}$ , which arise as consequences of strong coupling. The first one  $W_{C^- C^+}$  has a dependence  $\propto \cos^2 \theta \sin^2 \theta$  which makes it large for molecules with a detuning smaller than the Rabi coupling. A similar discussion applies to the products of rates on the cascades  $C^+ \rightarrow U_1 \rightarrow C^-$  and  $C^+ \rightarrow U_0^* \rightarrow C^-$ . They correspond to two-step relaxation processes  $C^+ \rightarrow C^-$  which are large when  $\cos^2 \theta \sin^2 \theta$  has its maximum value. These processes offer possibilities to explain a selection of strongly coupled molecules among a diverse population. The other non-radiative rates have smaller values  $W_{U_0 U_0^*} \sim 10^{12} \text{ s}^{-1}$  and  $W_{C_0 C^-} \sim 10^{12} \text{ s}^{-1} \gg \Gamma_{C_0 C^-}$ .

These orders of magnitude allow one to write down a simplified system of rate equations. The largest absorption rate is indeed the one  $A_{U_1 U_0}$  associated to the absorption from  $U_0$  to  $U_1$  and the main relaxation channel is then through non-radiative relaxation from  $U_1$  to  $C^-$ . The populations of the states  $C^+$  and  $U_0^*$  remain negligible at all times and can be ignored in the following simplified

system of solutions

$$\begin{aligned} [U_1](t) &\simeq \int_0^t dt' e^{-R_{U_1} t'} A_{U_1 U_0}(t-t') [U_0], \\ [C^-](t) &\simeq \int_{t_0}^t dt' e^{-R_{C^-} t'} W_{C^- U_1} [U_1](t-t'), \end{aligned} \quad (13)$$

where  $R_{U_1}$  and  $R_{C^-}$  are the total relaxation rates for states  $U_1$  and  $C^-$

$$\begin{aligned} R_{U_1} &\simeq \Gamma_{U_0 U_1} + W_{C^- U_1}, \\ R_{C^-} &\simeq \Gamma_{C_0 C^-} + W_{C_0 C^-}. \end{aligned} \quad (14)$$

The population of  $U_1$  follows the pumping rate (7), with a delay determined by  $R_{U_1}$ . As already stated, the population of  $U_0$  is not significantly depleted and can be considered as constant. The population of  $C^-$  follows the feeding from  $U_1$ , with a delay determined by  $R_{C^-}$ . As  $R_{U_1} \sim 5 \times 10^{13} \text{ s}^{-1}$  is  $\sim 50$  times larger than  $R_{C^-} \sim 10^{12} \text{ s}^{-1}$ , it follows that  $[U_1]$  reaches a quasi-stationary value  $A_{U_1 U_0} [U_0] / R_{U_1}$  after a very short time  $R_{U_1}^{-1} \sim 20 \text{ fs}$ . Then  $[C^-]$  shows a quasi-stationary behavior for a much longer time  $R_{C^-}^{-1} \sim 1 \text{ ps}$  during which it is by far the most populated excited state and determines all observables. This explains the main feature observed in the experiments, that is the extremely long lifetime of the lower dressed state  $C^-$ , which is much longer than that of other excited states.

## 7 Discussion

The decay of  $C^-$  is dominated by the internal vibrational relaxation whereas the radiative decay (fluorescence) is a negligible pathway. Even if the fluorescence rate is not suppressed, it is overwhelmed by the non-radiative rate [31]. This importance of the non-radiative decay with respect to the radiative one is confirmed by the small emission quantum yield measured at the level of strongly coupled molecules (numbers given below).

Meanwhile, the higher dressed state  $C^+$  is much shorter lived due to the extremely rapid vibrational decay to  $C^-$  and energy transfer to uncoupled molecules (see Fig. 3). The lifetime of  $C^+$  turns out to be less than 150 fs while the lifetime of  $C^-$  is of the same order, at resonance, than that of the bare molecule [18,26,27]. In fact, the strong asymmetry in the  $C^-$  and  $C^+$  lifetimes is a direct proof of the importance of the vibrational coupling for the decay process of the polaritons, as well as of the non-Markovian character of the associated relaxation. As also known for the lowest excited level of most molecules,  $C^-$  has a very long lifetime precisely because the vibrational overlap between the lowest excited level and the ground state is much smaller than between it and the higher excited states.

Let us discuss here two examples. For merocyanine strongly coupled ( $\Omega_R \sim 0.7 \text{ eV}$ ) to a Fabry-Perot cavity of low  $Q$ -factor ( $\sim 10$ ), the half-life of  $C^- \sim 10 \text{ ps}$

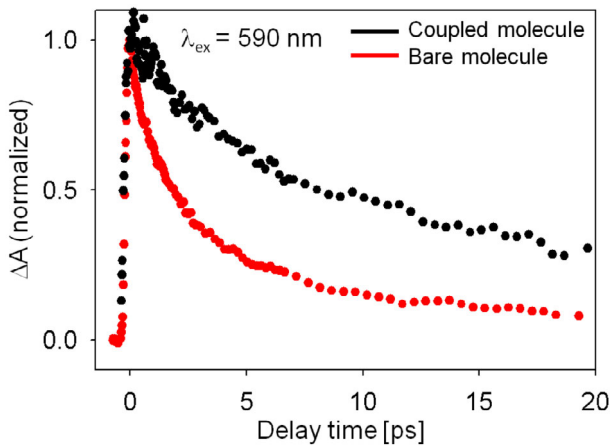


**Fig. 4.** Temporal evolution of the total change in absorption recorded immediately after a 150 fs pump pulse at 590 nm for a bare film of TDBC molecules (red data) and for TDBC molecules coupled to the cavity (black data; see Fig. 1b). After the pumping rise time, the relaxation appears exponential over this time scale, in agreement with equation (3). The half-life of  $C^- \sim 4$  ps (black) is thus longer than that of the bare molecule (red). At this time scale, the radiative lifetime ( $\sim 25$  fs) of the low  $Q$  cavity appears as instantaneous.

is much longer than the photon lifetime in the bare cavity ( $\Gamma_{U_0U_1}^{-1} \sim 25$  fs) while being shorter than that of bare molecules (30 ps) [26]. In the case of the TDBC J-aggregate strongly coupled ( $\Omega_R \sim 0.35$  eV) to a similar low  $Q$  cavity,  $C^-$  has a half-life of 4 ps, which is even longer than the 1 ps half-life of the bare organic material, as shown in Figure 4. Note that these lifetime values are the same whether  $C^-$  is excited resonantly or not. When the pump reaches higher electronic levels of uncoupled or coupled molecules, the same transient spectrum and lifetime are observed, confirming that  $C^-$  determines the observable because the population accumulates in this longest-lived state.

It is important to note that this measured long lifetime cannot be explained by a “bottleneck”-type effect, as involved at the level of strongly coupled inorganic systems [36]. Indeed, we do not observe any spectral shift in the transient signal for  $\tau > 150$  fs, whereas such spectral shifts should be expected if a “bottleneck” effect would play a role. This stresses again the remarkable difference between organic and inorganic systems.

We also emphasize that for both types of molecules, the quantum yields in the strong coupling regime are remarkably low. Indeed, for merocyanine, a highly efficient organic dye, the measured quantum yield associated with  $C^-$  falls below  $10^{-4}$  [26,27] while we measure for TDBC a fluorescence quantum yield  $\Phi_f \sim 8 \times 10^{-3}$  [31]. These measurements give access to the relaxation pathways occurring for  $C^-$  because  $\Phi_f = k_r / (k_r + k_{nr}) = k_r \tau_{C^-}$  where  $k_r$  and  $k_{nr}$  are, respectively, the radiative and non-radiative decay rates and  $\tau_{C^-}$  the lifetime of the  $C^-$  state. Low values of  $\Phi_f$  indicate that the non-radiative relaxation is the dominant decay pathway for  $C^-$ . In reference [31], values such as  $k_{nr} \sim 10^{12} \text{ s}^{-1} > 100k_r$  have been reported for

TDBC for instance due to a large number of vibrational modes available to transfer the population of the  $C^-$  state to the fundamental state.

It is also possible to measure the radiative rate  $k_r$  of a molecule from its absorption spectrum. This approach, together with the determination of the quantum yield, has provided a measure of the lifetime of the state [31]. Such measurements have been performed for TDBC and gave the remarkable result of a long  $C^-$  lifetime at the level of a few picoseconds. This is in a reasonable agreement with a direct transient absorption determination of the lifetime of  $C^-$  shown below (Fig. 4). In fact, molecules with high oscillator strength such as merocyanine and TDBC, have radiative rates at best  $\sim 10^9 \text{ s}^{-1}$  so that, given the observed  $C^-$  life times of the order of picoseconds, quantum yields are expected to be less than  $10^{-2}$ .

## 8 Conclusion

We have shown in this paper that the observed lifetimes of the polariton states are naturally explained in the non-Markovian relaxation approach proposed in the present paper. The lifetimes of the excited states are determined by vibrational relaxation phenomena and they are strongly affected by the large Rabi splitting which changes the overlaps of the vibrational reservoirs. In particular, the lifetime of the lower dressed state  $C^-$  is much longer than that of other excited states and its value is disconnected from that of the photon decay rate in the bare cavity, or of the relaxation rates of bare molecular states. This explains the main features observed in experiments and also opens new possibilities to influence chemical dynamics by controlling organic strong coupling.

The authors are grateful to Claude Cohen-Tannoudji, James A. Hutchison and Jean-Marie Lehn for fruitful discussions. This work was funded in part by the ERC (Grant No. 227577) and the ANR (Equipex Union).

## References

1. D.G. Lidzey, D.D.C. Bradley, M.S. Skolnick, T. Virgili, S. Walker, D.M. Whittaker, *Nature* **395**, 53 (1998)
2. T. Fujita, Y. Sato, T. Kuitani, T. Ishihara, *Phys. Rev. B* **57**, 12428 (1998)
3. P. Schouwink, H.V. Berlepsch, L. Dahne, R.F. Mahrt, *Chem. Phys. Lett.* **344**, 352 (2001)
4. N. Takada, T. Kamata, D.D.C. Bradley, *Appl. Phys. Lett.* **82**, 1812 (2003)
5. R.J. Holmes, S.R. Forrest, *Phys. Rev. Lett.* **93**, 186404 (2004)
6. J.R. Tischler, M.S. Bradley, V. Bulović, J.H. Song, A. Nurmikko, *Phys. Rev. Lett.* **95**, 036401 (2005)
7. P. Michetti, G.C. La Rocca, *Phys. Rev. B* **71**, 115320 (2005)
8. T.K. Hakala, J.J. Toppari, A. Kuzyk, M. Pettersson, H. Tikkanen, H. Kunttu, P. Törmä, *Phys. Rev. Lett.* **103**, 053602 (2009)

9. J. Bellessa, C. Bonnand, J.C. Plenet, J. Mugnier, *Phys. Rev. Lett.* **93**, 036404 (2004)
10. J. Dintinger, S. Klein, F. Bustos, W.L. Barnes, T.W. Ebbesen, *Phys. Rev. B* **71**, 035424 (2005)
11. S.A. Guebrou, C. Symonds, E. Homeyer, J.C. Plenet, Y.N. Gartstein, V.M. Agranovich, J. Bellessa, *Phys. Rev. Lett.* **108**, 066401 (2012)
12. T. Ambjarnsson, G. Mukhopadhyay, P.S. Apel, M. Käll, *Phys. Rev. B* **73**, 085412 (2006)
13. A. Berrier, R. Cools, C. Arnold, P. Offermans, M. Crego-Calama, S.H. Brongersma, J. Gomez-Rivas, *ACS Nano* **5**, 6226 (2011)
14. C. Ciuti, G. Bastard, I. Carusotto, *Phys. Rev. B* **72**, 115303 (2005)
15. T. Schwartz, J.A. Hutchison, C. Genet, T.W. Ebbesen, *Phys. Rev. Lett.* **106**, 196405 (2011)
16. J.A. Hutchison, A. Liscio, T. Schwartz, A. Canaguier-Durand, C. Genet, V. Palermo, P. Samori, T.W. Ebbesen, *Adv. Mater.* **25**, 2481 (2013)
17. A. Canaguier-Durand, E. Devaux, J. George, Y. Pang, J.A. Hutchison, T. Schwartz, C. Genet, N. Wilhelms, J.-M. Lehn, T.W. Ebbesen, *Angew. Chem. Int. Ed.* **125**, 10727 (2013)
18. J.H. Song, Y. He, A.V. Nurmikko, J. Tischler, V. Bulovic, *Phys. Rev. B* **69**, 235330 (2004)
19. G.P. Wiederrecht, J.E. Hall, A. Bouhelier, *Phys. Rev. Lett.* **98**, 083001 (2007)
20. A. Salomon, C. Genet, T.W. Ebbesen, *Angew. Chem. Int. Ed.* **48**, 8748 (2009)
21. P. Vasa, R. Pomraenke, G. Cirimi, E. De Re, W. Wang, S. Schwieger, D. Leipold, E. Runge, G. Cerullo, C. Lienau, *ACS Nano* **4**, 7559 (2010)
22. T. Virgili, D. Coles, A.M. Adawi, C. Clark, P. Michetti, S.K. Rajendran, D. Brida, D. Polli, G. Cerullo, D.G. Lidzey, *Phys. Rev. B* **83**, 245309 (2011)
23. Y.W. Hao, H.Y. Wang, Y. Jiang, Q.D. Chen, K. Ueno, W.Q. Wang, H. Misawa, H.B. Sun, *Angew. Chem. Int. Ed.* **50**, 7824 (2011)
24. V.M. Agranovitch, M. Litinskaia, D.G. Lidzey, *Phys. Rev. B* **67**, 085311 (2003)
25. M. Litinskaya, P. Reineker, V.M. Agranovich, *J. Lumin.* **110**, 364 (2004)
26. J.A. Hutchison, T. Schwartz, C. Genet, E. Devaux, T.W. Ebbesen, *Angew. Chem. Int. Ed.* **51**, 1592 (2012)
27. T. Schwartz, J.A. Hutchison, J. Leonard, C. Genet, S. Haacke, T.W. Ebbesen, *Chem. Phys. Chem.* **14**, 125 (2013)
28. C. Weisbuch, H. Bensity, R. Houdré, *J. Lumin.* **85**, 271 (2000)
29. C. Cohen-Tannoudji, S. Reynaud, *J. Phys. B* **10**, 345 (1977)
30. S. Reynaud, C. Cohen-Tannoudji, *J. Phys.* **43**, 1021 (1982)
31. S. Wang, T. Chervy, J. George, J.A. Hutchison, C. Genet, T.W. Ebbesen, *J. Phys. Chem. Lett.* **5**, 1433 (2014)
32. G.D. Scholes, *Annu. Rev. Phys. Chem.* **54**, 57 (2003)
33. R. Houdré, R.P. Stanley, M. Ilegems, *Phys. Rev. A* **53**, 2711 (1996)
34. P. Vasa, W. Wang, R. Pomraenke, M. Lammers, M. Maiuri, C. Manzoni, G. Cerullo, C. Lienau, *Nat. Photon.* **7**, 128 (2013)
35. P. Forn-Díaz, J. Lisenfeld, D. Marcos, J.J. García-Ripoll, E. Solano, C.J.P.M. Harmans, J.E. Mooij, *Phys. Rev. Lett.* **105**, 237001 (2010)
36. F. Tassone, C. Piermarocchi, V. Savona, A. Quattropani, P. Schwendimann, *Phys. Rev. B* **56**, 7554 (1997)